Rock Mechanics and Rock Engineering (2022) 55:5659–5669
https://doi.org/10.1007/s00603-022-02946-0

ORIGINAL PAPER

Mechanical Characterization and Creep Behavior of a Stone Heritage Material Used in Granada (Spain): Santa Pudia Calcarenite

Luisa María Gil-Martín[1] · Manuel Alejandro Fernández-Ruiz[2] · Enrique Hernández-Montes[1]

Received: 17 May 2022 / Accepted: 24 May 2022 / Published online: 25 June 2022

Abstract

Santa Pudia calcarenite was one of the most commonly used building materials in the construction of historical buildings in the city of Granada (Spain). As a result, Santa Pudia calcarenite has been mainly studied from a petrographical point of view in previous works. In this work, the mechanical properties of Santa Pudia calcarenite are studied. The main mechanical properties (compressive strength, elastic modulus and Poisson's ratio) were determined using the corresponding tests. Samples of Santa Pudia calcarenite were heated at 550 °C to study the effect of high temperatures on its compressive strength. Two different cooling methods were considered: air-cooling and water-cooling. Stress–strain curves of heated and non-heated samples were obtained from uniaxial compression tests. Creep is of great importance in the long-term structural assessment of historical buildings. To study the creep behaviour of Santa Pudia calcarenite, samples were subjected to uniaxial compressive tests at constant stress until the stabilization of the recorded strains was reached. Different rheological models were adjusted to the experimental results to simulate the long-term behaviour of the material studied. The instantaneous response to additional loadings on the samples (maintaining the long-term loading and deformation) were also studied. Results show that a Santa Pudia calcarenite specimen subjected to dead loads will suffer a higher instantaneous deformation against a sudden load than a non-preloaded specimen. This degradation effect can be particularly important in the case of a seismic evaluation of historical buildings.

Highlights

- The mechanical properties of Santa Pudia Calcarenite (SPC) are studied.
- The effect of high temperatures on the compressive strength of SPC is studied.
- Creep is of great importance in the long-term structural assessment of historical buildings.
- The creep behaviour of SPC is studied and different rheological models have been considered.

Keywords Calcarenite · Creep · Temperature · Compressive strength · Instantaneous response after creep

✉ Manuel Alejandro Fernández-Ruiz
manuelalejandro.fernandez@uca.es

Luisa María Gil-Martín
mlgil@ugr.es

Enrique Hernández-Montes
emontes@ugr.es

[1] Department of Structural Mechanics, University of Granada (UGR), Campus Universitario de Fuentenueva s/n., 18072 Granada, Spain

[2] Department of Industrial and Civil Engineering, Universidad de Cádiz (UCA), Campus Bahía de Algeciras, Avda. Ramón Puyol, s/n, 11201 Algeciras (Cádiz), Spain

1 Introduction

Stone can be considered to be one of the most important construction materials in historical buildings. The use of this natural material is closely related to the evolution of humanity, from the creation of primitive stone tools to the construction of striking heritage buildings. Knowledge of the mechanical behavior of historical building materials is a fundamental step in ensuring the preservation of historical buildings (Germinario et al. 2017; Scrivano and Gaggero 2020; Wang et al. 2020; Shabani et al. 2021). Santa Pudia Calcarenite (SPC) is a type of limestone widely used in the

construction of emblematic historical buildings in the city of Granada (Spain), such as the Cathedral, the Royal Hospital, the Palace of Carlos V, the Royal Chapel and the San Jerónimo Monastery (see Fig. 1).

Due to the importance of SPC in the cultural heritage of Granada, several works have been carried out related to this calcarenite stone. In Rodriguez-Navarro and Sebastian (1996), the influence of vehicle exhaust gases on the degradation of SPC was studied. A detailed work about the petrographic and physical characteristics of SPC was carried out in Molina (2015). On the other hand, the durability of SPC and the effectiveness of treatments for its enhancement have also been extensively studied in the related literature (Cultrone et al. 2007; Luque et al. 2008; Molina et al. 2011, 2013; Vázquez et al. 2013). In addition, a degradation model of SPC is proposed in (Jalón et al. 2020). In (Rodriguez-Navarro 1994), the alteration of different heritage building materials was studied, including the study of some mechanical properties of SPC such as its compressive, tensile, and flexural strength. Based on experimental data, Rodríguez-Navarro (Rodriguez-Navarro 1994) concluded that the compressive strength of SPC was approximately 10 times greater than Brazilian tensile strength.

As can be seen, much attention has been paid to the durability and petrographical properties of SPC, but comparatively less to its mechanical properties.

In this work, SPC is studied from a mechanical point of view to fill this gap.

The exposure of rocks to high temperatures (mainly due to a fire) can produce physical and chemical changes in their internal structure (Sirdesai et al. 2017; Jin et al. 2020). High temperature induces intergranular and intragranular micro-cracks in rocks. The main controlling parameters for the physical properties of rocks are the geometry and density of cracks and pores (Yavuz et al. 2010). Consequently, porosity, bulk density and the velocity of the propagation of ultrasonic waves are affected (Yavuz et al. 2010; Hong et al. 2012). From an engineering point of view, a key parameter for the use of stone as a building material is its uniaxial compressive strength. Different types of sandstones exposed to high temperatures were studied in Wu et al. (2005), where a slight decrease in compressive strength was observed in temperatures of up to 400 °C. However, an abrupt decline was observed between 400 and 600 °C (around 60% of the compressive strength of the non-heated samples). In Zhang et al. (2009), a downward trend in the compressive strength of sandstone was observed from 200 to 600 °C. The influence of temperature on the compressive strength of San Julian calcarenite (originally from Alicante, Spain) was studied in Brotóns et al. (2013b). Samples were heated at different temperatures ranging from 105 to 600 °C (Estevan et al. 2021). In addition, two different cooling methods were used: air-cooling and water-cooling. The results showed a decreasing trend in compressive strength with the increase in temperature (Brotóns et al. 2013b). Nevertheless, there are some works that have detected an initial hardening at temperatures between 200 and 400 °C (Rao et al. 2007; Ranjith et al. 2012). In Hong et al. (2012) a compilation of physical changes produced by temperature on sandstones from other scientific works is presented. Hong et al. conclude that the variations of the physical properties of sandstones can be too small to be ignored after thermal treatment in the order of 100–200 °C, but it normally becomes significant above treatment in the order of 400 or 500 °C. The influence of the pore structure on gas diffusion and permeability (Benavente and Pla 2018) and the relation between the static and dynamic elastic modulus (Brotons et al. 2016) in different building stones have also been studied. The rheology and time-dependent behavior are basic mechanical properties of rock materials (Sorace 1998; Li and Xia 2000) and masonry (Binda et al. 1991; Shrive et al. 1997). Creep behavior refers to the continued deformation under constant stress. It is necessary to take creep behavior into account when determining the long-term response of historical buildings, tunnels, dam abutments and in every case in which rocks support permanent loads. The creep phenomenon has been studied by several authors. In Weng et al. (2010), an elastic-viscoplastic creep model was proposed for weak rocks (specially oriented towards tunnel construction). The creep behavior of a particular type of calcarenite was studied in Brotóns et al. (2013a) using uniaxial compressive tests with a duration of 96 h. In Ding et al. (2017), the creep behavior of tight sandstone under different axial stresses was carried out. Finally, in Yang and Hu (2018) creep experiments were performed on red sandstones after different thermal treatments.

The deterioration of cultural heritage sites is one of the biggest challenges in conservation; aspects such as building technologies/materials and their structural response must be considered. The assessment of both the deterioration of mechanical properties due to extreme events and the

Fig. 1 San Jerónimo Monastery in Granada (Spain)

long-term response of heritage building materials is of great importance.

In this work, the mechanical properties of Santa Pudia calcarenite are studied. Basic mechanical properties such as uniaxial compressive strength, elastic modulus and Poisson's ratio were obtained from the corresponding tests (EN14580 2006; EN1926 2006). Some SPC samples were exposed to a high temperature (550 °C, in accordance with Hong et al. 2012) to determine its effect on the compressive strength and on the stress–strain curve of the material. Two different cooling methods were considered: air-cooling and water-cooling. The creep behavior of SPC was determined from prismatic samples subjected to a constant stress for around 15 days (the time at which the strains caused by the maintained load were stabilized). Once the creep had happened, all the specimens were subjected to an additional load to estimate the instantaneous elastic response of the SPC. This was done to obtain the current modulus of elasticity, applicable, for example, to a structure subjected to ground movements, when it is already deformed by permanent loads. Several rheological models were adjusted to the experimental results of SPC.

2 Materials and Methods

2.1 Materials Used

Santa Pudia calcarenite is a type of limestone that has been quarried for at least five centuries in Granada (Spain). All the samples of SPC tested in this work were taken from a quarry in Escúzar (a small village approximately 25 km southwest of the city of Granada). In Molina et al. (2011, 2013), Molina (2015), extensive work was carried out on the petrographical and physical characteristics of SPC obtained from the same quarry from which the samples used in this work were taken. SPC is a Tortonian bioclastic calcarenite composed of calcitic bioclasts and a small amount of siliceous fragments (Molina 2015). It is mainly composed of calcite (> 95%) and quartz (5%), with traces of dolomite, muscovite and goethite (Molina 2015). SPC presents an open porosity value of $32.8 \pm 2.3\%$ (Molina et al. 2013) and an apparent density of 1730 kg/m^3 (Molina et al. 2011). For more information about the petrographical and physical characteristics of SPC, the reader should consult (Molina et al. 2011, 2013; Molina 2015).

2.2 Uniaxial Compressive Strength

Ten cubic samples with sides of 50 mm were tested under uniaxial compression to obtain the compressive strength of SPC according to the European Standard EN 1926 (EN1926 2006). To meet the requirements on surface preparation, the specimens were finished on a surface grinder (especially the faces to which the load was applied). This surface preparation was also carried out for the rest of the specimens tested in the experimental campaign. Before the tests, all the specimens were dried at 70° until no mass change occurred. Then, the specimens were tested using a hydraulic actuator with a capacity of 1000 kN (see Fig. 2a). During the tests, the load was increased monotonically in load control with a rate of 0.5 MPa/s according to (EN1926 2006). Two LVDT linear transducers with a range of 10 mm were used to measure the axial deformation. The stress–strain (σ–ε) curve of each SPC cubic specimen was obtained from the uniaxial compression test. Special care was taken to collect a high number of readings from the post-peak part of the curve.

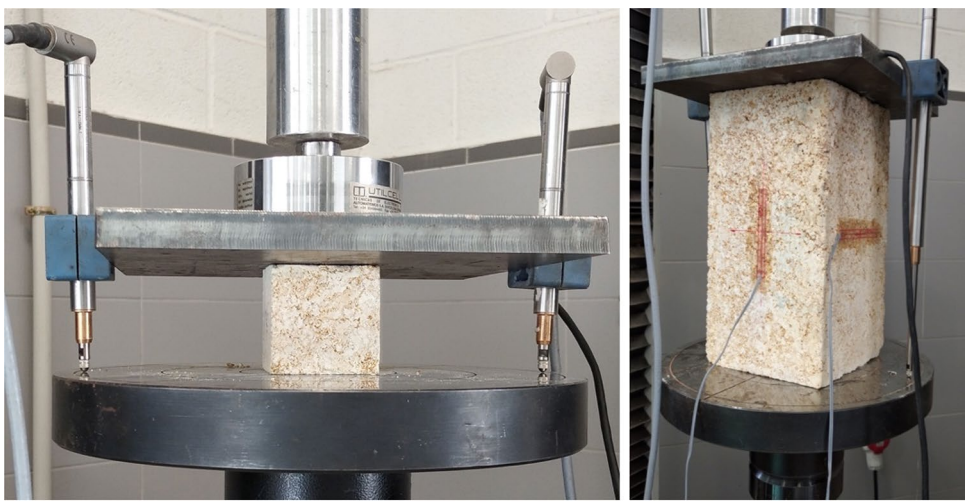

(a) (b)

Fig. 2 **a** Uniaxial compression and **b** elastic modulus test setup of SPC

2.3 Elastic Modulus

The elastic modulus and the Poisson's ratio of SPC was obtained from six prismatic specimens with dimensions of 120 × 120 × 240 mm according to the European Standard EN 14580 (EN14580 2006). The specimens were heated until a temperature of 70º was reached and temperature was kept until no mass change (EN1926 2006). Then, two strain gauges (one longitudinal and one transversal) were attached to each specimen (see Fig. 2b). During the tests, the load was increased monotonically in load control at a rate of 0.5 MPa/s. According to (EN14580 2006), before carrying out the elastic modulus test and to define its load pattern, the compressive strength had to be determined in accordance with (EN1926 2006).

2.4 Creep Tests

To study the rheological behavior of SPC when submitted to a stress level close to that found in real service conditions, a constant compressive load of around 9000 N was applied for a certain time to nine prismatic specimens with dimensions of 120 × 120 × 450 mm. The above compressive load corresponds to a stress of around 20% of the average unconfined compressive strength of SPC. The load was introduced with a lever using a beam to transfer the load to each sample (see Fig. 3). This mechanism allowed the application of a constant load until a stabilization of deformation was observed (which happens at around 15 days). Both LVDT linear transducers with a range of 10 mm and dial gauges (0.01 mm reading) were used to record the deformation of the samples. A load cell placed on the top of each specimen was used to measure the load applied.

Fig. 3 Configuration of the creep tests

2.5 Heating Process

To study the influence of temperature on the stress–strain curve and on the compressive strength of SPC, ten cubic samples with sides of 50 mm, which had been previously subjected to a high temperature, were tested under uniaxial compression. The heating process was as follows: SPC samples were introduced into an oven until the target temperature (550 °C) was reached. Later, the SPC specimens were cooled in two different ways to study the influence of the different cooling methods: water-cooling and air-cooling (five specimens for each case). Water-cooled specimens (SPC-W) were cooled by water immersion for 5 min and then they were air cooled at laboratory temperature for two days. However, the air-cooled specimens (SPC-A) were air cooled at laboratory temperature for two days. Finally, all the SPC specimens were heated until they reached a temperature of 70° before testing, to eliminate water content (EN1926 2006). Ten SPC non-heated samples (SPC-0) were also tested for reference.

2.6 Instantaneous Response to Additional Loadings After Creep Tests

To predict the response of the SPC material under a sudden load, such as an earthquake or an impact in service conditions (i.e., concomitant with a maintained load such as dead loads), an instantaneous additional compressive load was applied to the specimens after creep took place, while maintaining the original load.

To analyze the influence of the level of stress in the elastic response of SPC, loads ranging between 10% and 25% of the value of the average compressive strength were applied to the specimens until stabilization of deformation (see Fig. 3). Once the deformations stopped increasing, the additional instantaneous increment of the stress applied ranged between 1% and 3% of the compressive strength of SPC (i.e., between 0.05 and 0.15 MPa).

The values of stress and strain associated with these additional loads were recorded, and the ratio between the measured stress increment and its corresponding strain increment were considered as the post-creep elastic modulus of the SPC (named E'_{SPC}).

3 Results and Discussion

3.1 The Influence of Temperature on Compressive Strength and on Stress–Strain Curves

The results of the uniaxial compressive strength tests of SPC-0, SPC-A and SPC-W are shown in Table 1. Compressive strength was computed as the average of the maximum compressive stress

Table 1 Compressive strength of SPC-0, SPC-A and SPC-W specimens (values in MPa)

SPC-0	SCP-A	SPC-W
4.82 ± 1.58	3.09 ± 0.93	2.61 ± 0.46

registered during the tests. The uniaxial compressive strength of SPC decreases with high temperatures for both the air-cooled and water-cooled procedures. Table 1 shows a decrease of 35.9% in SPC-A and of 45.8% in SPC-W when compared with SPC-0. As can be seen in Table 1, the fast cooling of SPC-W samples has the greatest impact on compressive strength. This is because the sudden water-cooling generates micro-cracks that connect pores (Brotóns et al. 2013b), having a negative effect on the compressive strength of the specimen. On the other hand, the slow cooling (SPC-A) leads to an expansion of the pores produced during the heating process (Brotóns et al. 2013b), which is reflected in a smaller decrease in compressive strength. The lower expected value of compressive strength according to the European Standard EN 1926 (EN1926 2006) was 3.55 MPa for SPC-0, 2.38 for SPC-A and 2.32 for SPC-W, respectively. These results are in line with the ones presented in (Brotóns et al. 2013b), where a decrease of 35% and 50% in air-cooled and water-cooled samples heated at 550 °C, respectively, was observed.

Figure 4 shows the average stress–strain (σ–ε) curves of SPC-0, SPC-A and SPC-W (including standard deviation). The strain corresponding to each stress level was computed using the piston stroke and LVDT readings and the stress was computed as the axial load introduced by the hydraulic actuator divided by the cross-sectional area of the samples (initial).

As can be seen in Fig. 4, the σ–ε curves show a similar ultimate strain. However, the value of the strain at peak stress is lower in the case of SPC-0 in comparison with both SPC-A and SPC-W. The descending branch of the σ–ε curves was also affected by temperature. Both SPC-A and SPC-W curves showed a descending branch with a slope that was smaller than SPC-0, resulting in better ductility. These results are in line with the ones presented in (Sygała et al. 2013), where brittle fractures turn into a ductile sandstone destruction model when the temperature increases.

3.2 Static Elastic Modulus and Poisson's Ratio

The average value of the static elastic modulus of SPC obtained from the mechanical procedure described in (EN14580 2006) was 11595.19 ± 1974.19 MPa. On the other hand, the Poisson's ratio estimated from the recorded strains was 0.32 ± 0.12. Both results are in line with the results reported in (Molina et al. 2011, 2013; Molina 2015).

3.3 Creep

Figure 5 shows the average creep strain, as function of time, for the tested samples when subjected to a maintained compressive load such that it causes a compressive stress of around 20% of the average compressive strength of SPC in the specimens. The time-dependent strain was obtained by subtracting the instantaneous elastic strain from the total axial strain. Besides the average curve, Fig. 5 also shows the standard deviation corresponding to the statistical analysis of the nine specimens tested. At a certain moment of the tests (at approximately 280 h) the difference between the readings of the nine tests was reduced, and consequently, the standard deviation was also reduced.

In this piece of work, different rheological models are considered to estimate the long-term creep behavior of SPC.

3.3.1 CEB-FIP Model Code 2010 Creep Model

The creep model proposed by the CEB-FIP Model Code 2010 (MC2010 (FIB 2012)) was originally conceived for concrete. However, in this work, it is used for SPC. The strain due to creep is as follows (FIB 2012):

$$\varepsilon_{cc}(t,t_0) = \frac{\sigma_c(t_0)}{E_{ci}}\varphi(t,t_0) \tag{1}$$

In Eq. (1) t is the time, t_0 the time when the load was applied, σ_c the compressive stress, E_{ci} the elastic modulus at 28 days and φ the creep coefficient. The expression of the creep coefficient proposed by MC2010 (FIB 2012) can be summarized with the expression shown in Eq. (2).

$$\varphi(t,t_0,RH,h) = \left(1+\frac{1-\frac{RH}{100}}{0.1\,h^{1/3}}\left(\frac{35}{f_{cm}}\right)^{0.7}\right)\left(\frac{35}{f_{cm}}\right)^{0.2}\frac{16.8}{\sqrt{f_{cm}}}\frac{1}{0.1+t_0^{0.2}} \times\left(\frac{t-t_0}{1.5\,h\left(1+\left(\frac{1.2\,RH}{100}\right)^{18}\right)+250\left(\frac{35}{f_{cm}}\right)^{0.5}+(t-t_0)}\right)^{0.3} \tag{2}$$

In Eq. (2), RH is the relative humidity of the ambient environment in %, h is the notional size of the member in mm ($h = 2A_c/u$, where A_c is the cross-section in mm^2 and u is the perimeter of the section in contact with the atmosphere in mm), f_{cm} is the mean compressive strength at 28 days in MPa. In Eq. (2), t and t_0 must be expressed in days. As the creep model proposed by MC2010 (FIB 2012) was used for concrete, a very old type of concrete has been considered to simulate SPC.

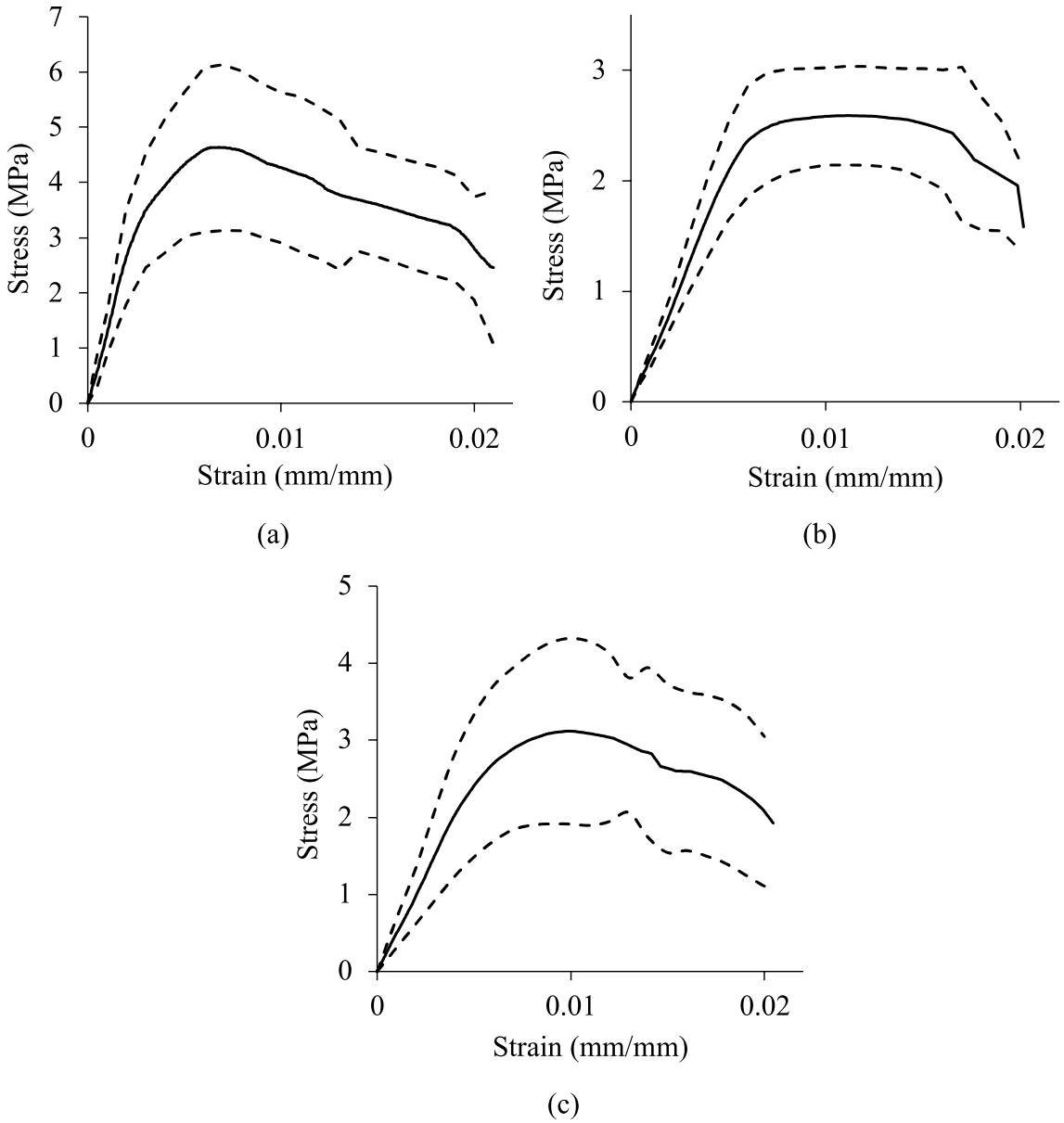

Fig. 4 Average stress–strain curves of all the SPC samples tested (black curves). Dashed black curves correspond to the standard deviation of compressive stress. **a** SPC-0; **b** SPC-W; **c** SPC-A

Therefore, the mechanical properties do not vary over time. A value of $t_0 = 10000$ days is considered, as it was done in Brotóns et al. (2013a). The values of compressive strength (f_{cm}) and elastic modulus (E_{ci}) at 28 days were the ones obtained from the mechanical tests (4.82 and 11595.19 MPa, respectively) and $RH = 70\%$. Figure 5 shows the average creep experimental curve together with the creep model proposed by MC2010 (FIB 2012) adapted for SPC. It can be seen that the MC2010 creep model provides a good approximation of the experimental creep curves. Consequently, the MC2010 creep model initially conceived for concrete seems to be applicable to sandstone. However, it is necessary to confirm this for different stress conditions.

3.3.2 Other Rheological Models

There are some widely used models for creep, such as the Burgers model (A.E.N.D.C. 1935), the Kelvin model (Flugge 1967) and the fractional Maxwell model (Blair

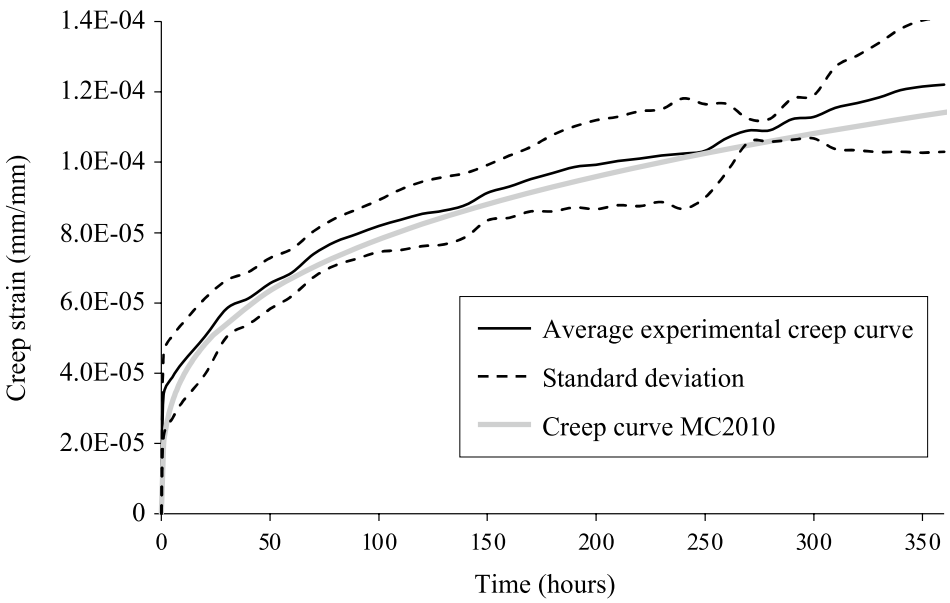

Fig. 5 Average experimental creep curve (continuous black curve, dashed black curves correspond to the standard deviation) and creep curve proposed by MC2010 (gray line)

1947). The minimal rheological model suitable for physical processes is the Maxwell model (Maxwell 1867). The Maxwell model is graphically composed of a Hooke spring and a Newton dashpot (representing the damping). Consequently, this model describes the deformation behavior with only a single characteristic time scale consisting of a constant strain rate and an exponential type of stress relaxation (Ding et al. 2017). The Maxwell model can be modified by adding more Hooke springs and/or Newton dashpots to simulate more complex physical interactions. Examples of these modifications are the rheological models represented in Fig. 6. As it can be seen in Fig. 6a, the Burgers model consists of two Hooke springs and two Newton dashpots, the Kelvin model is constructed with two Hooke springs and one Newton dashpot (see Fig. 6b). The fractional Maxwell model consists of one Hooke spring and one Scott Blair dashpot (Blair 1947) (see Fig. 6c), which is qualitatively different from the Maxwell model. The fractional Maxwell model is a good candidate for describing complex creep dynamics (Ding et al. 2017) and it is suitable for describing the behavior of a system with an infinite number of relaxation modes (Ding et al. 2017). The total strain of the rheological models shown in Fig. 6a–c are indicated in Eqs. (3), (4) and (5) respectively.

$$\varepsilon(t) = \sigma_0 \left(\frac{1}{E_0} + \frac{1}{E_1} \left(1 - \mathrm{e}^{\left(-\frac{E_1}{\eta_1} t \right)} \right) + \frac{t}{\eta_0} \right) \tag{3}$$

$$\varepsilon(t) = \sigma_0 \left(\frac{1}{E_0} + \frac{1}{E_1} \left(1 - \mathrm{e}^{\left(-\frac{E_1}{\eta_1} t \right)} \right) \right) \tag{4}$$

$$\varepsilon(t) = \sigma_0 \left(\frac{1}{E_0} + \frac{1}{\eta_0^{\alpha}} \frac{t^{\alpha}}{\Gamma(1+\alpha)} \right) \tag{5}$$

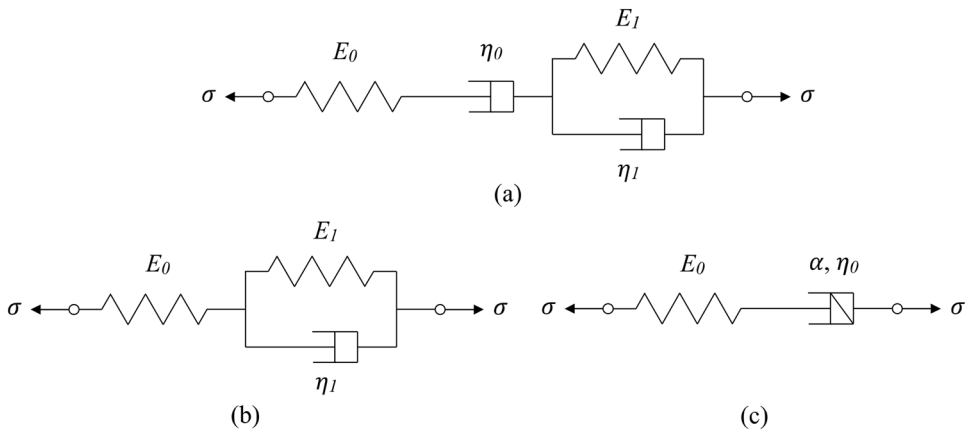

Fig. 6 Burgers (**a**), Kelvin (**b**) and fractional Maxwell (**c**) rheological models

In Eq. (5), Γ is the Gamma function. For a given stress σ_0, the corresponding total strain ε can be expressed as the sum of the elastic strain ε_e (which is time independent) and the time-dependent strain ε_t. In all the models shown in Fig. 6, the elastic strain is $\varepsilon_e = \sigma_0/E_0$, as a result of Hooke's law. In the experimental data shown in Fig. 5, the elastic strain has been removed (i.e., only the time-dependent strain is considered) this is why the Hooke spring with E_0 that appears in all the rheological models shown in Fig. 6 has not been considered when fitting the experimental data to these models. The parameters of the rheological models and the goodness of fit R^2 corresponding to the average experimental creep curve shown in Fig. 5 can be seen in Table 2.

Despite a high value of R^2 being obtained for all the models considered, it is obvious that in Fig. 7 the fractional Maxwell model is the one which best agrees with the experimental data over the full range of time in comparison with the Burgers and Kelvin models (as in Ding et al. 2017). The results in Fig. 7 show that the Burgers model provides a better fit to the experimental results than the Kelvin model. This is because the Burgers model is a more complex rheological model than the Kelvin one (see Fig. 6), which is the simplest viscoelastic model, and so it may have some limitations when describing creep.

Table 2 Fitting of creep results with the studied rheological models

Model	Parameters	R^2
Burgers (Eq. 4)	$\eta_0 = 1.227 \times 10^7$ GPa s	0.998
	$E_1 = 9.741$ GPa	
	$\eta_1 = 3.371 \times 10^5$ GPa s	
Kelvin (Eq. 5)	$E_1 = 5.516$ GPa	0.989
	$\eta_1 = 1.225 \times 10^6$ GPa s	
Fractional Maxwell (Eq. 6)	$\eta_0 = 300.73$ GPa s^{α}	0.999
	$\alpha = 0.293$	

3.4 Immediate Response of SPC Specimens After Creep

The results of the instantaneous response of SPC specimens after creep in terms of the ratio between stress and strain increments corresponding to the additional load applied, E'_{SCP} (i.e. $E'_{SCP} = \Delta\sigma/\Delta\varepsilon$), are represented in Fig. 8. Horizontal axis of Fig. 8 represents the maintained load to which the specimen was being subjected the specimen when the instantaneous load was applied. Trend line in Fig. 8 shows

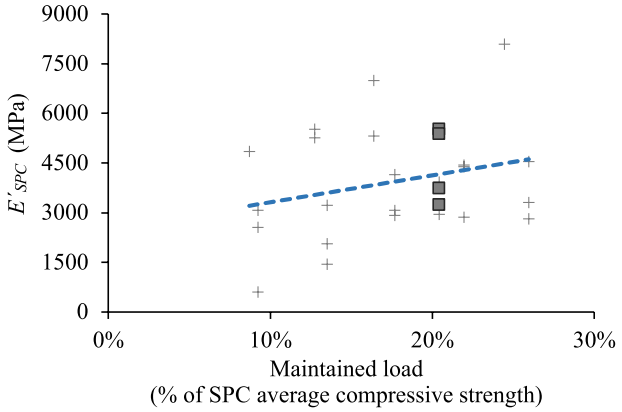

Fig. 8 Instantaneous response of SPC after creep versus the maintained load

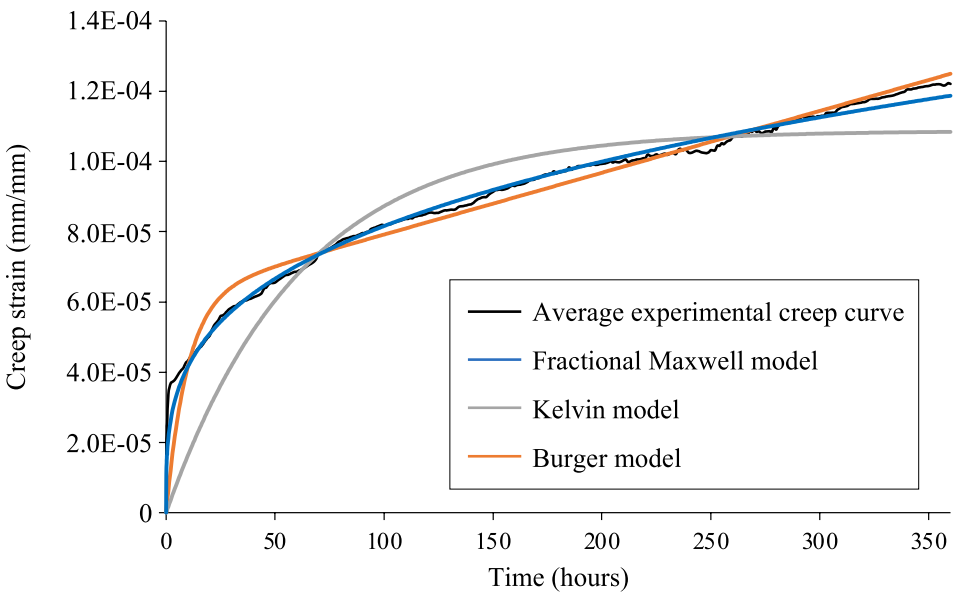

Fig. 7 Fitting average experimental creep curve to three rheological models

Table 3 Elastic modulus E_{SCP} (EN14580 2006), post-creep elastic modulus E'_{SCP} and effective elastic modulus $E_{SCP,eff}$ of Santa Pudia calcarenite

E_{SPC}	E'_{SPC}	$E_{SPC,eff}$
11,595.19 ± 1974.19	4399.36 ± 1028.34	3451.72 ± 587.69

that the instantaneous response seems to be more stiffen for higher sustained loads.

The average value of E'_{SCP} ($=\Delta\sigma/\Delta\varepsilon$) corresponding to a maintained compressive stress of around 20% of the compressive strength of SPC and $\Delta\sigma = 0.05$ MPa was 4399.4 ± 1028.3 MPa. In Table 3, the initial elastic modulus of these SPC specimens has also been collected to allow comparison (squares in Fig. 8).

In practice, in concrete structures and for service-stress levels, the response of the structure considering time-dependent effects is approximated as a linear elastic problem taking into account the age adjusted effective modulus defined in Eq. (6). Using the same line of reasoning, in the case of SPC, the experimental creep coefficient is 2.36 at the end of the tests. This creep coefficient has been computed using Eq. (1) with the average value of the experimental creep strain at the end of the tests (see Fig. 5), the elastic modulus E_{SPC} (see Table 3), and the average compressive stress applied during the tests. Therefore, the effective modulus of elasticity of SPC ($E_{SPC,eff}$) is 3451.72 MPa.

$$E_{SPC,eff} = \frac{E_{SPC}}{1+\varphi} \tag{6}$$

$E_{SPC,eff}$ is also collected in Table 3.

So, among the mechanical properties of the calcarenite, a stiffness degradation effect has been found. The stiffness degrading coefficient in concrete structures is dependent on the maximum displacement (Aschheim et al. 2019). This particular experiment shows that this stiffness degradation should also depend on the loading time. For a seismic analysis of a construction with heritage value, the real loading conditions should be reproduced using tests to evaluate the current elastic modulus.

Table 3 and Fig. 8 show that, for a given applied compressive load, calcarenite stone subjected to dead loads will suffer a greater instantaneous deformation than a non-preloaded specimen.

4 Conclusions

In this work, the mechanical properties and the creep behavior of Santa Pudia calcarenite are studied. Based on the results obtained in this research, the following conclusions can be drawn:

1. The uniaxial compressive strength of SPC (4.82 ± 1.58 MPa) showed a decrease with high temperatures for both air-cooled (3.09 ± 0.93 MPa) and water-cooled (2.61 ± 0.46 MPa) procedures (of 35.9% and 45.8%, respectively, in comparison with SPC-0).
2. The stress–strain (σ–ε) curves of Santa Pudia calcarenite at ambient temperature (SPC-0), and cooled using two different procedures (air-cooled (SPC-A) and water-cooled (SPC-W)) after heating at 550 °C showed a similar ultimate strain. In addition, SPC-A and SPC-W σ–ε curves showed a descending part with a slope smaller than SPC-0, resulting in better ductility.
3. The static elastic modulus and Poisson's ratio of SPC are 11595.19 ± 1974.19 MPa, and 0.32 ± 0.12, respectively.
4. The creep model proposed by the CEB-FIP Model Code 2010 has been applied to SPC. SPC has been considered to be similar to very old concrete. The MC2010 creep model provided a good approximation of the experimental creep curve.
5. Well-known rheological models, such as the Burgers, Kelvin and fractional Maxwell models, have been fitted to the experimental results. Fitted parameters are provided for each model to be applied in the modelling SPC creep behavior. The fractional Maxwell model showed the best fit to the experimental results over the full range of time.
6. The deterioration of the mechanical properties due to extreme events and the long-term response of heritage building materials such as SPC is of great importance in the structural assessment of historical buildings. In this work an instantaneous additional compressive load was introduced at the end of the creep tests (while maintaining the original load). The elastic modulus after creep tests was calculated as the ratio between increments of stress and strains: $E'_{SPC} = 4399.36 \pm 1028.34$ MPa. A stiffness degradation effect can be observed if the values of E_{SPC} and E'_{SPC} are compared. Consequently, SPC specimens subjected to maintained loads suffer a bigger instantaneous deformation than non-preloaded specimens. Seismic analysis needs to account for this effect.

Funding Open Access funding provided thanks to the CRUE-CSIC agreement with Springer Nature. This work is part of the HYPERION project (https://www.hyperion-project.eu/). HYPERION has received funding from the European Union Framework Programme for Research and Innovation (Horizon 2020) under grant agreement no. 821054.

Declarations

Conflict of Interest The authors declared that there is no conflict of interest.

References

AENDC (1935) First report on viscosity and plasticity. Nature 136:697–699. https://doi.org/10.1038/136697a0

Aschheim M, Hernández-Montes E, Vamvatsikos D (2019) Design of reinforced concrete buildings for seismic performance: practical deterministic and probabilistic approaches. Taylor & Francis, CRC Press

Benavente D, Pla C (2018) Effect of pore structure and moisture content on gas diffusion and permeability in porous building stones. Mater Struct Constr 51:1–14. https://doi.org/10.1617/s11527-018-1153-8

Binda L, Anzani A, Gioda G (1991) An analysis of the time dependent behaviour of masonry walls. In: 9th Int. brick/block masonry conference, Berlin, pp 1058–1067

Blair GS (1947) The role of psychophysics in rheology. J Colloid Sci 2:21–32. https://doi.org/10.1016/0095-8522(47)90007-X

Brotóns V, Ivorra S, Tomás R, Benavente D (2013a) Study of creep behavior of a calcarenite: San Julián´s stone (Alicante). Mater Constr 63:581–595. https://doi.org/10.3989/mc.2013.06412

Brotóns V, Tomás R, Ivorra S, Alarcón JC (2013b) Temperature influence on the physical and mechanical properties of a porous rock: San Julian' s calcarenite. Eng Geol 167:117–127. https://doi.org/10.1016/j.enggeo.2013.10.012

Brotons V, Tomás R, Ivorra S et al (2016) Improved correlation between the static and dynamic elastic modulus of different types of rocks. Mater Struct Constr 49:3021–3037. https://doi.org/10.1617/s11527-015-0702-7

Cultrone G, Sebastia E, Ortega Huertas M (2007) Durability of masonry systems: a laboratory study. Constr Build Mater 21:40–51. https://doi.org/10.1016/j.conbuildmat.2005.07.008

Ding X, Zhang G, Zhao B, Wang Y (2017) Unexpected viscoelastic deformation of tight sandstone: insights and predictions from the fractional Maxwell model. Sci Rep 7:1–11. https://doi.org/10.1038/s41598-017-11618-x

EN14580 (2006) Natural stone test methods. Determination of elastic modulus. Comité Européen de Normalisation, Brussels, Belgium

EN1926 (2006) Natural stone test methods. Determination of uniaxial compressive strength. Comité Européen de Normalisation, Brussels, Belgium

Estevan L, Baeza FJ, Varona FB, Ivorra S (2021) Evaluation of the mechanical response of calcarenite specimens confined with fiber reinforced polymers after high temperature exposure. J Build Eng 42:102504. https://doi.org/10.1016/j.jobe.2021.102504

FIB (2012) Model Code 2010—final draft. vol 1. Fib bulletin no. 65. International Federation for Structural Concrete, Lausanne

Flugge W (1967) Viscoelasticity. Blaisdell Publishing Co., New York

Germinario L, Siegesmund S, Maritan L, Mazzoli C (2017) Petrophysical and mechanical properties of Euganean trachyte and implications for dimension stone decay and durability performance. Environ Earth Sci 76:1–21. https://doi.org/10.1007/s12665-017-7034-6

Hong T, Kempka T, Neng-Xiong X, Ziegler M (2012) Physical properties of sandstones after high temperature treatment. Rock Mech Rock Eng 45:1113–1117

Jalón ML, Chiachío J, Gil-Martín LM, Hernández-Montes E (2020) Probabilistic identification of surface recession patterns in heritage buildings based on digital photogrammetry. J Build Eng. https://doi.org/10.1016/j.jobe.2020.101922

Jin P, Hu Y, Shao J et al (2020) Influence of temperature on the structure of pore-fracture of sandstone. Rock Mech Rock Eng 53:1–12. https://doi.org/10.1007/s00603-019-01858-w

Li Y, Xia C (2000) Time-dependent tests on intact rocks in uniaxial compression. Int J Rock Mech Min Sci 37:467–475

Luque A, Cultrone G, Sebastián E, Cazalla O (2008) Effectiveness of stone treatments in enhancing the durability of bioclastic calcarenite in (Granada, Spain). Mater Constr 58:115–128. https://doi.org/10.3989/mc.2008.41607

Maxwell JC (1867) On the dynamical theory of gases. Philos Trans R Soc 157:49–88

Molina E (2015) Influencia de la textura, del sistema poroso y del acabado superficial en la durabilidad de areniscas y travertino explotados en Andalucía y utilizados en construcción. PhD Thesis, University of Granada

Molina E, Cultrone G, Sebastián E et al (2011) The pore system of sedimentary rocks as a key factor in the durability of building materials. Eng Geol 118:110–121. https://doi.org/10.1016/j.enggeo.2011.01.008

Molina E, Cultrone G, Sebastián E, Alonso FJ (2013) Evaluation of stone durability using a combination of ultrasound, mechanical and accelerated aging tests. J Geophys Eng. https://doi.org/10.1088/1742-2132/10/3/035003

Rodriguez-Navarro C (1994) Causas y mecanismos de alteración de los materiales calcáreos de las Catedrales de Granada y Jaén. PhD Thesis. University of Granada

Ranjith PG, Viete DR, Chen BJ, Perera MSA (2012) Transformation plasticity and the effect of temperature on the mechanical behaviour of Hawkesbury sandstone at atmospheric pressure. Eng Geol 151:120–127

Rao Q, Wang Z, Xie H, Xie Q (2007) Experimental study of mechanical properties of sandstone at high temperature. J Cent South Univ Technol 14:478–483

Rodriguez-Navarro C, Sebastian E (1996) Role of particulate matter from vehicle exhaust on porous building stones (limestone) sulfation. Sci Total Environ 187:79–91

Scrivano S, Gaggero L (2020) An experimental investigation into the salt-weathering susceptibility of building limestones. Rock Mech Rock Eng 53:5329–5343. https://doi.org/10.1007/s00603-020-02208-x

Shabani A, Kioumarsi M, Zucconi M (2021) State of the art of simplified analytical methods for seismic vulnerability assessment

of unreinforced masonry buildings. Eng Struct 239:112280. https://doi.org/10.1016/j.engstruct.2021.112280
Shrive NG, Sayed-Ahmed EY, Tilleman D (1997) Creep analysis of clay masonry assemblages. Can J Civ Eng 24:367–379
Sirdesai NN, Singh TN, Pathegama Gamage R (2017) Thermal alterations in the poro-mechanical characteristic of an Indian sandstone—a comparative study. Eng Geol 226:208–220. https://doi.org/10.1016/j.enggeo.2017.06.010
Sorace S (1998) Effects of initial creep conditions and temporary unloading on the long-term response of stones. Mater Struct Constr 31:555–562. https://doi.org/10.1007/bf02481538
Sygała A, Bukowska M, Janoszek T (2013) High temperature versus geomechanical parameters of selected rocks—the present state of research. J Sustain Min 12:45–51. https://doi.org/10.7424/jsm130407
Vázquez P, Alonso FJ, Carrizo L et al (2013) Evaluation of the petrophysical properties of sedimentary building stones in order to establish quality criteria. Constr Build Mater 41:868–878. https://doi.org/10.1016/j.conbuildmat.2012.12.026
Wang Y, Pei Q, Yang S et al (2020) Evaluating the condition of sandstone rock-hewn cave-temple façade using in situ non-invasive techniques. Rock Mech Rock Eng 53:2915–2920. https://doi.org/10.1007/s00603-020-02063-w
Weng MC, Tsai LS, Hsieh YM, Jeng FS (2010) An associated elastic–viscoplastic constitutive model for sandstone involving shear-induced volumetric deformation. Int J Rock Mech Min Sci 47:1263–1273. https://doi.org/10.1016/j.ijrmms.2010.08.022
Wu Z, Qin B, Chen L, Luo Y (2005) Experimental study on mechanical character of sandstone of the upper plank of coal bed under high temperature. Chinese J Rock Mech Eng 24:1863–1867
Yang SQ, Hu B (2018) Creep and long-term permeability of a red sandstone subjected to cyclic loading after thermal treatments. Rock Mech Rock Eng 51:2981–3004. https://doi.org/10.1007/s00603-018-1528-8
Yavuz H, Demirdag S, Caran S (2010) Thermal effect on the physical properties of carbonate rocks. Int J Rock Mech Min Sci 47:94–103. https://doi.org/10.1016/j.ijrmms.2009.09.014
Zhang L, Mao X, Lu A (2009) Experimental study on the mechanical properties of rocks at high temperature. Sci China E Technol Sci 52:641–646